Retraction

Retraction: Volumetric quantification in ovarian pathology using abdomino-pelvic computed tomography (*J. Phys.: Conf. Ser.* **1414** 012020)

O Valbuena[1], M I Vera[2], M Vera[1], E Gelvez-Almeida[1], Y Huérfano[2], M Borrero[1], J Salazar-Torres[1], W Salazar[1]

[1]Facultad de Ciencias Básicas y Biomédicas, Universidad Simón Bolívar, Cúcuta, Colombia
[2]Facultad de Ciencias, Universidad de Los Andes, San Cristobal, Venezuela

Published 06 February 2020

This paper was retracted by IOP Publishing on 6th February 2020, as it was a duplicate of a paper in another conference volume.

Volumetric quantification in ovarian pathology using abdomino-pelvic computed tomography

O Valbuena[1], M I Vera[2], M Vera[1], E Gelvez-Almeida[1], Y Huérfano[2], M Borrero[1], J Salazar-Torres[1], and W Salazar[2]

[1] Facultad de Ciencias Básicas y Biomédicas, Universidad Simón Bolívar, Cúcuta, Colombia

[2] Facultad de Ciencias, Universidad de Los Andes, San Cristobal, Venezuela

E-mail: m.avera@unisimonbolivar.edu.co

Abstract. Pathological ovary is categorized into cystic tumors, solid tumors and mixed, according to the content of the affected ovary. Accordingly, the degree of benignity or malignity thereof is established. The imaging study for the preliminary morphological assessment of PO is ultrasound, in its pelvic and transvaginal modalities, for which well-established criteria are available. Once the ultrasound findings suggest malignancy, complementary studies such as abdominal-pelvic tomography images and tumor markers are requested. This type of images has challenging problems called noise, artifacts and low contrast. In this paper, in order to address these problems, a computational technique is proposed to characterize a pathological ovary. To do this, a thresholding and the median and gradient magnitude filters are applied, preliminarily, to complete the preprocessing stage. Then, during the segmentation, the algorithm of region growing is used to extract the three-dimensional morphology of the pathological ovary. Using this morphology, the volume of the pathological ovary is calculated and it allows selecting the surgical-medical behavior to approach this kind of ovary. The validation of the proposed technique indicates that the results are promising. This technique can be useful in the detection and monitoring the diseases linked to pathological ovary.

1. Introduction

The ovaries are two nodular bodies located one on either side of the uterus, attached to the broad ligament, and situated close to the lateral pelvic wall in the ovarian fossa [1].

On the other hand, the survival rate of epithelial ovarian cancer (EOC) is approximately 35% – 40% despite maximal treatment efforts, highlighting a need for stratification biomarkers for personalized treatment [2].

The modalities of medical imaging play a crucial role in the diagnosis of ovary lesions. Multilayer computed tomography (MSCT) and ultrasound technique are is the primaries diagnostic methods for ovary tumors. Additionally, the segmentation of ovary tumors is a problem of great interest because the three-dimensional (3D) segmentation of these tumors from MSCT images is a prerequisite for computer-assisted diagnosis, treatment planning and cancer control of ovary. The main imperfection of MSCT images is the stair-step artifact, which dramatically deteriorates the appearance of such objects and can affect the dimensions especially of small structures present in the images acquired under this modality [4]. This is a real problem due the ovaries are a very small anatomical structures and this type of artifact can affect severely the associated information with the ovary.

Several works related to the segmentation of ovary or ovary tumor, which are presented at next. In this sense, Cigale and Zazula performing the ovarian segmentation in ultrasound images using cellular neural networks obtaining an accuracy of 70% [3]. Ramya and Kiruthika propose a technique to detect ovary follicles present in ultrasound images. For this, they incorporate discrete wavelet transform based k-means clustering and they report an accuracy of 96.11% based on structural similarity method [4]. Sonigo, *et al.* show a strategy based on deep learning to detect and to count ovary follicles in mouse ovary and they affirm that this strategy has an accuracy of 91.36% [5].

In this paper, the main purpose is to generate a semi-automatic technique (SAT) for pathological ovary (PO) segmentation, in MSCT images. This technique is based on the application of a filter bank (thresholding, median and gradient magnitude filters) and region growing technique in order to generate the 3D PO morphology. This bank is necessary for address the problems of the aforementioned imperfections of MSCT images. This technique can be useful in the detection and monitoring PO for establishing the main actions oriented to address the pathologies associated with PO.

2. Methodology

2.1. Dataset
A three-dimensional MSCT database was used, which has a voxel number of 512 x 512 x 70. Manual segmentation of the ovary by a ginecologist is also available.

2.2. Computational strategy proposed
In Figure 1, a schematic diagram is presented. It synthesizes the computational algorithms that make up the SAT for the segmentation of the human ovary. In this figure, the MSCT dataset matches with the dataset described in the 2.1 section of this paper. The other elements, shown in Figure 1, will be explained in the sections 2.2.1 and 2.2.2.

Figure 1. Block diagram of the proposed strategy.

2.2.1 Pre-processing. The main steps of this stage are: (i) Thresholding filter. Two thresholds linked to ovary detection were considered to isolate ovary in MSCT datasets. The thresholding method, used in this article, considers a histogram for threshold selection [6]. (ii) Median filter. A median image (M_I) is generated processing each original image (O_I) with a median filter [7]. The role of this filter is to address the noise present in the images. The tuning parameter of this filter is the size of the neighbourhood [8]. (iii) Gradient magnitude filter (GMF). In this work, an approach based on finite differences was used for GMF computational implementation [9]. This filter generates a smoothed version, called GM_I, calculating the three-dimensional gradient magnitude of M_I, using the mathematical model given by Equation (1).

$$GM_I = \left(\left(\frac{\partial M_I}{\partial i}\right)^2 + \left(\frac{\partial M_I}{\partial j}\right)^2 + \left(\frac{\partial M_I}{\partial k}\right)^2 \right)^{1/2}, \tag{1}$$

being: i, j, k the spatial directions in which the gradient is calculated and $\left(\frac{\partial M_I}{\partial i}, \frac{\partial M_I}{\partial j}, \frac{\partial M_I}{\partial k}\right)$. It is important to note that the computational cost (time of calculations) of the continuous model for GMF, given by the Equation (1), is very expensive. By this reason an approach based on central finite differences is used, in this paper, for modelling computationally the GMF [10].

2.2.2 Segmentation. In this stage the region growing technique is applied. Region growing technique (RG). The RG partitions an image (f) into regions (Ri) whose voxels are connected according to certain predefined criteria based on connectivity and similarity of the image. The most popular predefined criterion is given by Equation (2) [10].

$$\left| f(i, j, k) - \mu_{R_i} \right| < m\sigma_{R_i} \tag{2}$$

The RG needs a seed voxels into an initial neighborhood (Iv) being: $f(i, j, k)$ the gray levels of Iv, μ_{R_i} the average gray levels of a Iv of arbitrary shape and size, k an arbitrary scalar and σ_{R_i} the standard deviation of an arbitrary neighborhood of Iv. The Equation (2) represents the most popular predefined criterion due its simplicity and effectiveness.

In this point, it is necessary to notice that the RG tuning parameters are the initial neighborhood size (r) and k parameter that controls the amplitude of the range of intensities considered to accept or reject a voxel in a region. Such parameters must undergo a tuning process. During the tuning process, the PO segmented is compared with the manual segmentation traced by a ginecologist. The Ds is used in order to estimate the difference or matching between these structures [12].

3. Results
First, we present qualitative results using original and preprocessed images in two-dimensional (2D) and 3D views. Then the quantitative results are shown considering mainly the results accuracy and optimal parameters obtained by the algorithms present in the proposed SAT.

3.1. Qualitative results
Figure 2 shows a 2D view of both the original image and the processed images after applying the proposed technique to the dataset considered.
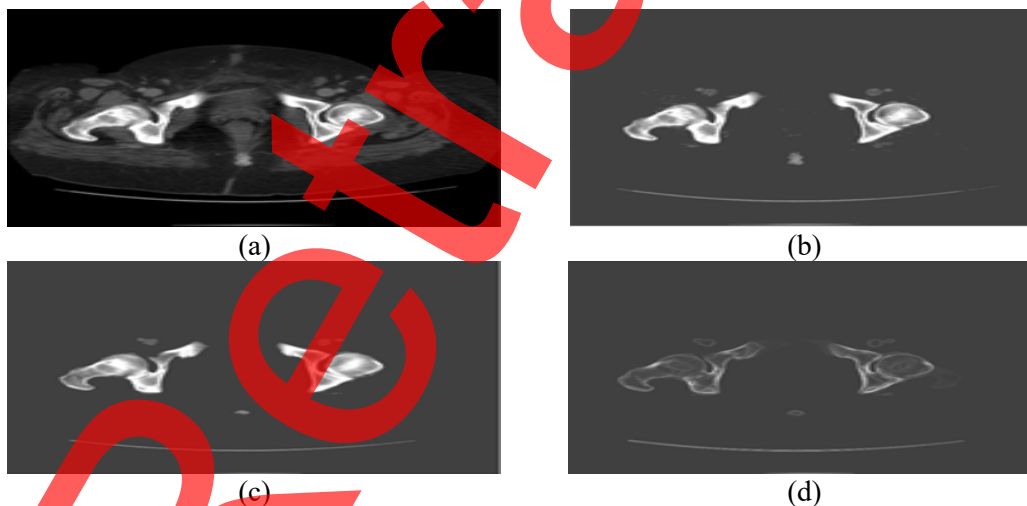

Figure 2. Preprocessing stage results; (a) original image, (b) thresholded image, (c) median image, (d) gradient magnitude image.

In Figure 2, we can observe the effects generated by filter bank application. A qualitative analysis revels that the considered filters generated high quality images reducing the noise and producing a high contrast between the anatomical structures. In Figure 2(a), we can observe the excellent performance of gradient magnitude filter for generating the contours of aforementioned structures. The threshold filter eliminates non-important anatomical structures and gives an adequate split image (see Figure 2(b)). The median filter generates an almost-free noise image that facilities the PO

segmentation (see Figure 2(c)); whereas the Figure 3(b) shows the enhancement contours linked to the pathological ovarian.

On the other hand, Figure 3 illustrates the results of the segmentation process developed using region growing technique. In this figure, we can observe an excellent representation of segmented kidney stone morphology in both 2D and 3D views.

(a) (b)
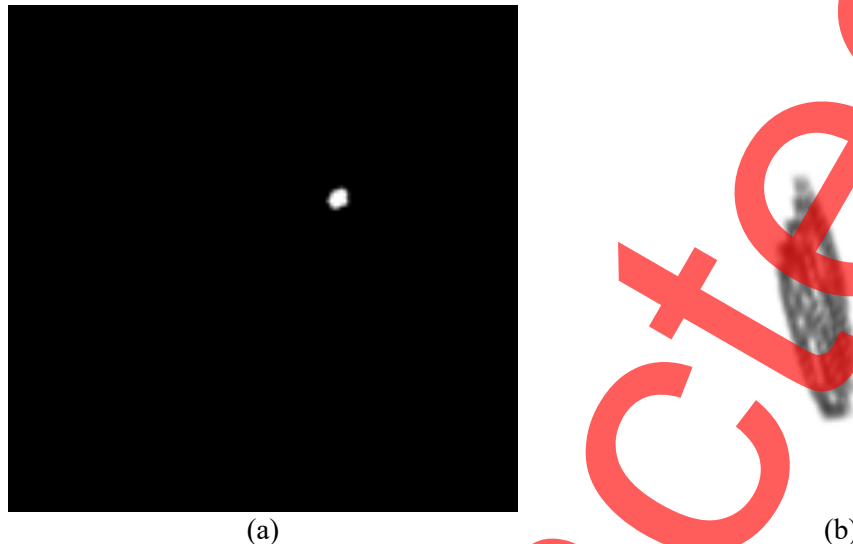
Figure 3. Pathological ovary segmented: (a) 2D view, (b) 3D view.

3.2. Quantitative results

When the tuning process was performed the PO was characterized considering its volume. So, the volume occupied by the semi-automatic segmented PO was 8.41 cm^3; while the volume, reported by the clinical expert, (obtained considering the manual segmentation) was 8.59 cm^3. The percentage relative error, considering these volumes, was 12.1%. This error represents an accuracy of 87.9%. Additionally, the maximum Dice coefficient generated was 0.82. This result allowed establishing the optimal parameters, of the computational algorithms that make up the proposed technique, which are presented below: a) Median filter: the size of the kernel was corresponding with (3x3x3). b) Region growing: r = 1 and k = 4.50. Additionally, the Table 1 shows comparative information about the accuracy obtained both in this paper and in others researches, reported in the specialized literature.

Table 1. Comparison using accuracy values for kidney stone segmentation.

Authors	Technique	Accuracy (%)
Cigale, *et al.* [3]	Cellular neural networks	70.00
Ramya, *et al.* [4]	k-means and wavelet transform	96.11
Sonigo, *et al.* [5]	Deep learning	91.36
Valbuena, *et al.* (Our technique)	SAT	87.90

The information analysis presented in Table 1, let us to affirm that SAT was outperform by the results reported by Ramya, *et al.* [4] and Sonigo, *et al.* [5]; whereas the computational technique proposes in this paper generated a higher accuracy value than that reported by Cigale, *et al.* [3]. It is important to notice that the techniques mentioned in Table 1 the reported in [5] is based on smart operators that belong to the deep learning context. According with the literature, these techniques exhibit an excessive computational time during the training stage; while our technique is very efficient and let us obtain results with a similar precision that the deep learning techniques when it is intend performing the PO segmentation.

4. Conclusions

A semi-automatic technique, available for detecting pathological ovary in a precise and efficient manner, has been presented. This technique was based in the application of thresholding, median and gradient magnitude filters in order to address the noise problem; whereas the region growing technique was applied for generating the 3D PO morphology, presents in MSCT images.

On the other hand, it is expected that the segmentation generated by the proposed method can be useful to promote, deepen and potentiate the study of the real anatomy of the structures linked to the ovaries. In the immediate future it is planned to validate the proposed technique with a significant number of databases in order to estimate the robustness of the aforementioned technique.

The three-dimensional representation of PO is useful for the detection and monitoring of ovaries diseases; as well as for the planning of medical treatments and clinical-surgical procedures linked to pathologies associated with the human ovaries.

References

[1] Blaustein A 1977 Anatomy and histology of the human ovary *Pathology of the female genital tract* ed Blaustein A (New York: Springer) Chapter 15 p 438
[2] Lu H, Arshad M, Thornton A, Avesani G, Cunnea P, CurryE, Kanavati F, Liang J, Nixon K, Williams S T, Ali Hassan M, Bowtell D D L, Gabra H, Fotopoulou C, Rockall A and Aboagye E O 2019 A mathematical-descriptor of tumor-mesoscopic-structure from computed-tomography images annotates prognostic and molecular-phenotypes of epithelial ovarian cancer *Nature Communications* **10** 764
[3] Cigale B and Zazula D 2004 Segmentation of ovarian ultrasound images using cellular neural networks *International Journal of Pattern Recognition and Artificial Intelligence* **18(4)** 563
[4] Ramya M and Kiruthika V 2014 Automatic segmentation of ovarian follicle using k-means *Fifth International Conference on Signal and Image Processing* (Bangalore: IEEE)
[5] Sonigo C, Jankowski S, Yoo O, Trassard O, Bousquet N, Grynberg M, Beau I and Binart N 2018 High-throughput ovarian follicle counting by an innovative deep learning approach *Scientific Reports* **8** 13499
[6] Pratt W 2007 *Digital image processing* (New York: John Wiley & Sons Inc)
[7] González R and Woods R 2001 *Digital image processing* (New Jersey: Prentice Hall)
[8] Petrou M and Bosdogianni P 2003 *Image processing the fundamentals* (New York: John Wiley & Sons Inc)
[9] Huérfano Y, Vera M, Mar A and Bravo A 2019 Integrating a gradient–based difference operator with machine learning techniques in right heart segmentation *Journal of Physics: Conference Series* **1160** 012003
[10] Burden R and Faires D 2010 *Numerical analysis* (Mexico: Cengage Learning)
[11] Saénz F, Vera M, Huérfano Y, Molina V, Martínez L, Vera MI, Salazar W, Gelvez E, Salazar J, Valbuena O, Robles H, Bautista M and Arango J 2018 Brain Hematoma Computational Segmentation *Journal of Physics: Conference Series* **1126** 012071
[12] Dice L 1945 Measures of the amount of ecologic association between species *Ecology* **26(3)** 29